Pierre Auger Note: GAP-2002-029

Optical Calibration of the Auger Fluorescence Telescopes

John A.J. Matthews
University of New Mexico,
New Mexico Center for Particle Physics,
Albuquerque, NM 87131, USA

July 22, 2002
Revised: August 20, 2002

Submitted to:
Proceedings SPIE Conference on *Astronomical Telescopes and Instrumentation*
22-28 August 2002, Waikoloa, Hawaii, USA

Optical Calibration of the Auger Fluorescence Telescopes

John A.J. Matthews[a] for the Pierre Auger Observatory Collaboration[b]

[a]New Mexico Center for Particle Physics, University of New Mexico, Albuquerque, NM 87131
[b]Observatorio Pierre Auger, Av. San Martin Norte 304, (5613) Malargue, Argentina

ABSTRACT

The Pierre Auger Observatory is optimized to study the cosmic ray spectrum in the region of the Greisen-Zatsepin-Kuz'min (GZK) cutoff, i.e. cosmic rays with energies $\sim 10^{20}$eV. Cosmic rays are detected as extensive air showers. To measure these showers each Auger site combines a 3000sq-km ground array with air fluorescence telescopes into a hybrid detector. Our design choice is motivated by the heightened importance of the energy scale, and related systematic uncertainties in shower energies, for experiments investigating the GZK cutoff. This paper focuses on the optical calibration of the Auger fluorescence telescopes. The optical calibration is done three independent ways: an absolute end-to-end calibration using a uniform, calibrated intensity, light-source at the telescope entrance aperture, a component by component calibration using both laboratory and in-situ measurements, and Rayleigh scattered light from external laser beams. The calibration concepts and related instrumentation are summarized. Results from the 5-month *engineering array* test are presented.

Keywords: Optical calibration, air fluorescence telescopes, UV LED, laser, xenon flash lamp, cosmic rays

1. INTRODUCTION

The Pierre Auger experiment studies cosmic rays in the region of the Greisen-Zatsepin-Kuz'min (GZK) cutoff. The existence (or not) of events above the GZK cutoff[1] emphasizes the importance of a well understood energy scale and well understood energy resolution for the Auger events.

A subset of all showers observed by Auger[2] will be measured by both the ground array and fluorescence detector (FD) telescopes. These special *hybrid* events[3] will be used to set the shower energy scale, based on the fluorescence detector determination of the shower energies, and to measure the shower energy resolution for the experiment. Consequently, the fluorescence measurement errors must be well understood. The largest fluorescence measurement uncertainties come from uncertainties in the atmospheric corrections,[4] from the calibration of the fluorescence telescopes, and from the fluorescence yield.[5] This paper focuses on the calibration of the fluorescence telescopes.

2. FLUORESCENCE DETECTOR OPTICAL CALIBRATION

The fluorescence light from the extensive air shower will be captured by the fluorescence telescopes, focused on cameras subdivided into 440 pixels, and digitized.[6] The telescope calibration provides the conversion between digitized signal, in ADC units, and photons incident on the 3.80m^2 telescope aperture. As the air fluorescence signal is collected over a range of wavelengths, $300 < \lambda < 420$nm, the telescope calibration is also a function of the wavelength of the photons. We then denote the calibration *efficiency*, for the i^{th}-pixel in the j^{th}-telescope, by: $\epsilon_{ADC}(\lambda)_{i,j}$. The units of ϵ_{ADC} are (ADC/photon).

A cross-section of one of the Auger fluorescence telescopes is shown in Fig. 1. The 2.2m diameter telescopes are a simple Schmidt system. UV filters[7] are installed in the entrance aperture to serve as a window and to exclude light with wavelengths > 420nm. Just inside the UV filter is a ring of (Schmidt) corrector elements covering radii of $0.85m < r < 1.1m$. Light is focused by a large 3.9m x 3.9m spherical mirror (needed to accommodate the $30° \times 30°$ field of view). The camera contains 440 photo-multiplier tubes (PMT)s. The cracks between PMTs are covered by reflective triangular inserts, termed Mercedes. These act like Winston cones and

Further author information: (Send correspondence to John A.J. Matthews)
John A.J. Matthews: E-mail: johnm@dot.phys.unm.edu, Telephone: 1 505 277 2077

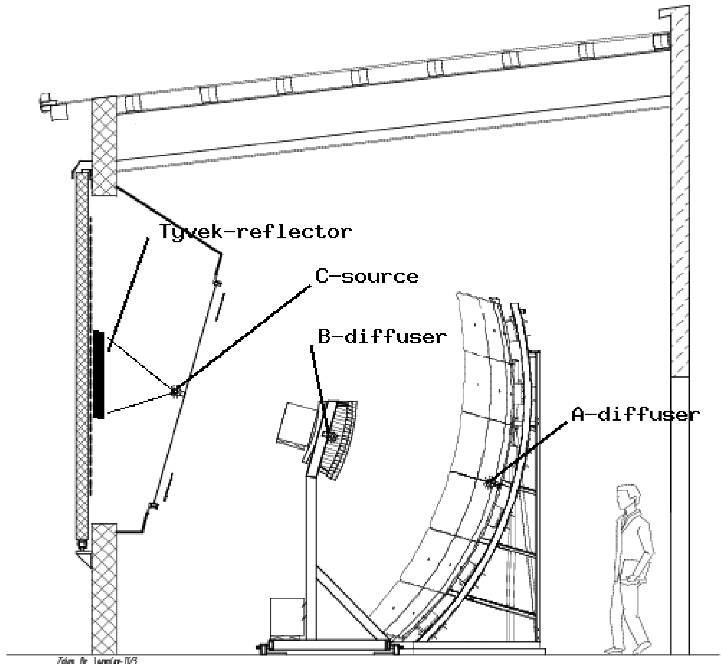

Figure 1. Schematic of the Auger fluorescence telescopes. Also shown are components of the relative optical calibration system: A-, B- and C-pulsed light sources. In this figure the telescope doors are closed to show the location of the TYVEK reflectors during C-source calibrations.

minimize variations in the camera response as the light image of the air shower moves across the face of the camera.[8]

The combined efficiency for all of these components must be known and changes in the efficiencies with time must be tracked. This calibration task has been broken down into two separate sub-tasks:

- absolute calibrations which are infrequent, and
- relative calibrations which are frequent.

The relative calibrations are to monitor time dependent changes between absolute calibrations. The absolute calibrations are done in three separate ways:

- *piece-by-piece* estimate,
- *Rayleigh* scattering from 355nm pulsed laser[9] beam(s),[10]
- flat-field *drum illuminator*(s) with 375 ± 12nm LED[11] pulsed source.

The *Rayleigh* and *drum illuminator* calibrations provide an absolute, end-to-end calibration of the fluorescence telescopes. By absolute we mean that the flux of photons on the telescope aperture is independently measured and known to an absolute precision: nominally $\sim 5\%$. By end-to-end we mean that the calibration procedure includes all efficiencies and geometrical effects. The end-to-end calibration procedure measures the ADC/photon efficiency, $\epsilon_{ADC}(\lambda_{source})_{i,j}$, at wavelength λ_{source} in one step.

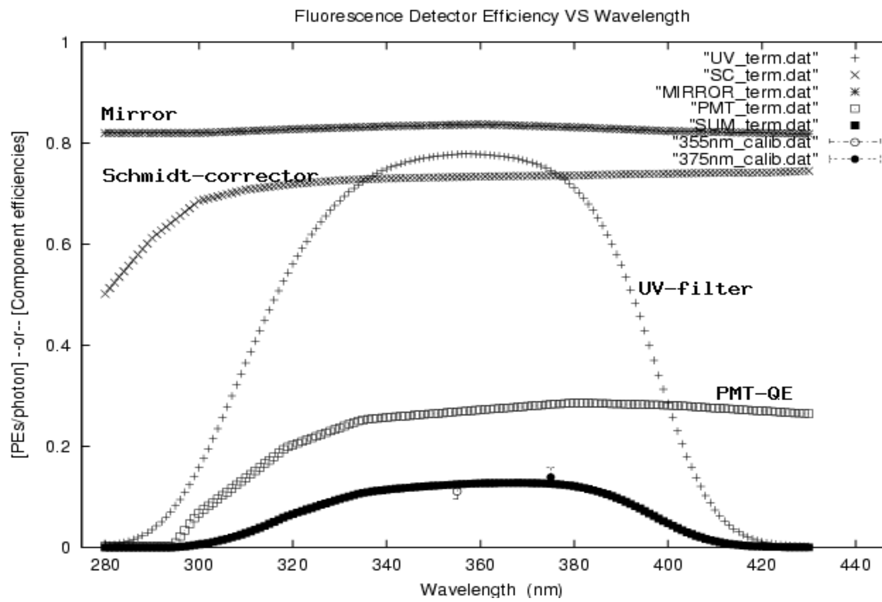

Figure 2. The predicted efficiency, $\epsilon_{PE}(\lambda)$, for producing a photo-electron per incident photon is shown as the solid-box points (lowest of the 5 curves) *versus* wavelength for Auger telescope-4. The model is for photons averaged over the angular acceptance of the telescope. Major contributors to the efficiency are also shown, where the *Schmidt-corrector* contribution includes the combined effect of the corrector ring and the camera shadow. See Fig. 9 for details on plotting the *Rayleigh* and *drum illuminator* absolute calibration results, points with error-bars, on this figure.

2.1. Absolute Optical Calibration

The absolute calibration of each of the Auger fluorescence telescopes should be known to a precision of $\sim 5\%$. To achieve this will not be easy. Significant progress to this goal was made during the fall of 2001 and winter of 2002 when 2 prototype fluorescence telescopes (denoted telescope-4 and -5) were operated in conjunction with $\sim$ 40 ground array detectors at the Pierre Auger Southern Observatory near Malargue Argentina. This was called the *engineering array* test. The goal of the test was to collect and reconstruct 50 $\sim$ 100 *hybrid* cosmic ray showers to provide the final proof-of-design and proof-of-implementation for the experiment. The *engineering array* test provided the first opportunity to carry out all three of the planned absolute calibration procedures.

2.1.1. *Piece-by-piece* Calibration

The *piece-by-piece* calibration estimated the ADC/photon efficiency by combining the efficiencies of each telescope-component with a ray-tracing program to include geometrical aperture, vignetting and shadowing effects. The component efficiencies came from measurements done on the individual pieces used in building each telescope.

In the *piece-by-piece* calibration the ADC/photon efficiency is factored into two components:

$$\epsilon_{ADC}(\lambda)_{i,j} \quad = \quad \epsilon_{PE}(\lambda)_{i,j} \quad \cdot \quad g_{i,j} \tag{1}$$

where: $\epsilon_{PE}(\lambda)_{i,j}$ is the efficiency for producing a photo-electron per incident photon (PE/photon) in a given pixel and $g_{i,j}$ is the electronics gain (ADC/PE) for each pixel. An example of the predicted efficiency, $\epsilon_{PE}(\lambda)$, for telescope-4 in the *engineering array* test is shown in Fig. 2. The electronics gain was evaluated using for example the relative calibration system (details below). Typical values were $\sim$ 1.8 ADC/PE[12].[13] The *piece-by-piece* calibration uncertainty was estimated at $\sim 20\%$ dominated by systematics including: aging of the various transmission or reflection surfaces (after characterization), simplicity of the ray-tracing simulation and uncertainties in our current evaluations of the electronics gains.

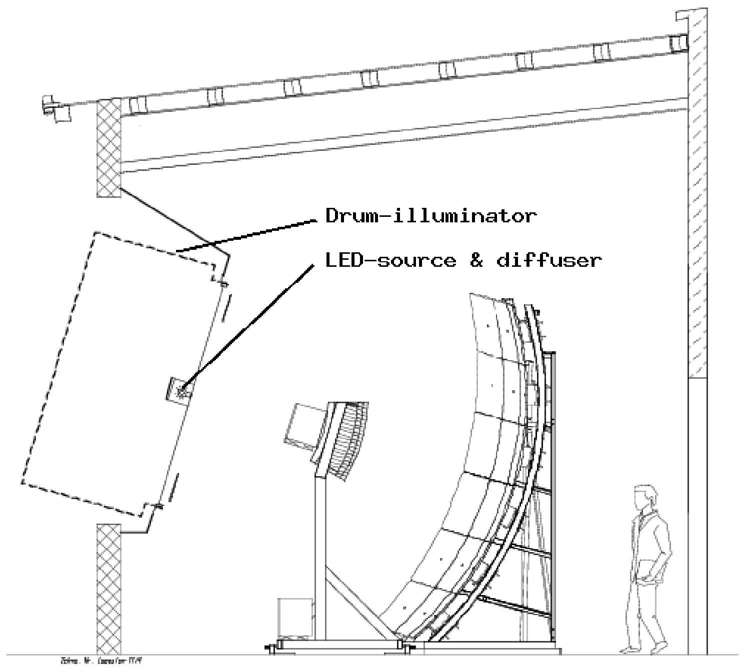

Figure 3. Schematic of *drum illuminator* positioned at the entrance aperture of one of the Auger fluorescence telescopes. The *drum illuminator* includes a LED-source and diffuser (light directed into the *drum*), TYVEK on the sides and rear surfaces of the drum, and 0.38mm thick Teflon (diffuser) on the front (light output) surface.

While the *piece-by-piece* calibration was the least precise of the three calibrations it provided a detailed model for the wavelength dependence of the calibration. It also provided an overall cross check of the *Rayleigh* and/or *drum illuminator* calibrations; see Figs. 2 and 9.

2.1.2. *Rayleigh* Calibration

In the *Rayleigh* calibration, a 355nm laser[9] was positioned a few kilometers from the fluorescence telescope to be calibrated. The laser was directed near-vertical and the pulse to pulse intensity monitored[14] to a precision of $\sim 5\%$. Light was scattered from the beam by Rayleigh scattering (on the molecular atmosphere) and by Mie scattering (on aerosols in the atmosphere). The scattered light was then used to calibrate the fluorescence telescope. The scattered light must be corrected for atmospheric attenuation and for the fraction of light scattered by aerosols. Both the atmospheric attenuation and aerosol corrections were minimized by choosing nights with few aerosols: *e.g.* with aerosol attenuation lengths > 40km. Furthermore the Mie:Rayleigh fraction was minimized by viewing the scattered light at scattering angles, θ, where the aerosol differential scattering cross section is smallest, *viz.* $100° < \theta < 150°$. These angles occur for near-vertical laser shots viewed by the fluorescence telescopes.

Absolute calibrations obtained for telescope-4 were: 5.1 photons/ADC[15] and 4.9 photons/ADC.[16] These results are compared with the *piece-by-piece* estimates in Figs. 2 and 9.

2.1.3. *Drum Illuminator* Calibration

In the *drum illuminator* calibration a drum-shaped, diffused, pulsed, light-source was positioned at the entrance aperture of the telescope under calibration, see Fig. 3. The *drum illuminator* provided rather uniform illumination over the entrance aperture of the telescope. A calibrated PMT measured the absolute light flux to a precision of $\sim 5\%$ before each telescope calibration.[17] To correct for small non-uniformities in the *drum* illumination, the *drum* was characterized at several viewing angles using a CCD camera. The CCD data were then parameterized to simulate the *drum illuminator* deviations from perfect, uniform illumination of a telescope.[18]

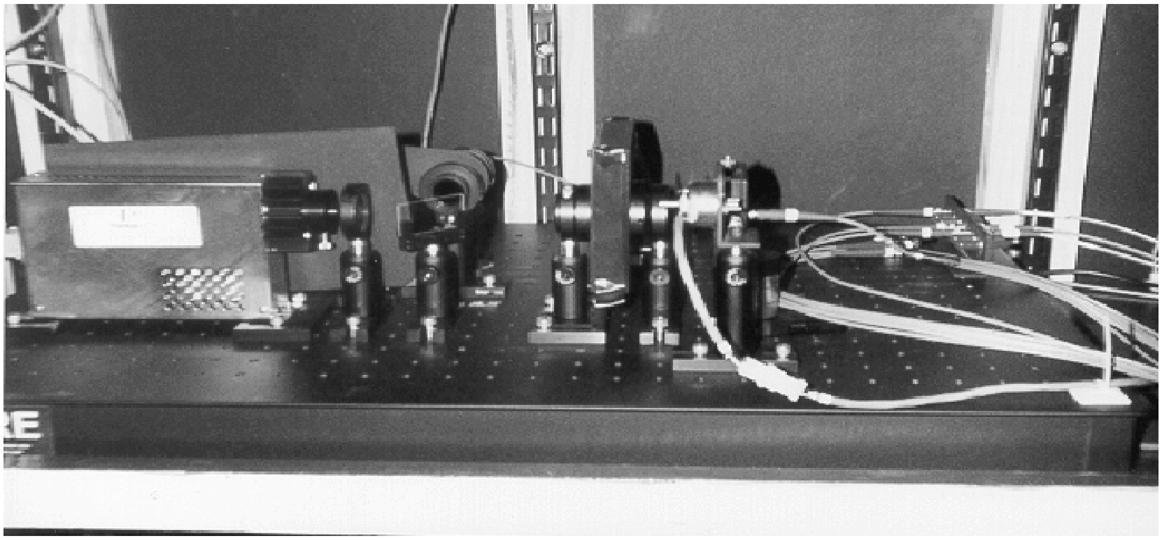

Figure 4. Photograph of one of the three optical calibration light sources at the (Los Leones) fluorescence detector site near Malargue Argentina. The optical calibration light sources mount on a 18" × 30" optical bread-board[23] which are in-turn supported on simple wall-mounted shelves.

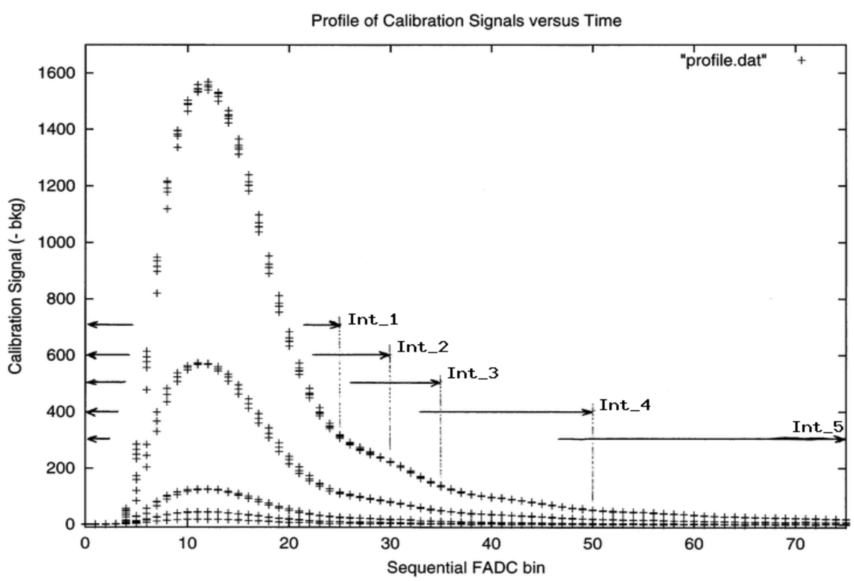

Figure 5. Typical light pulses from the "A"-source. Each time bin is 100nsec. The different intensities correspond to different neutral density filters. The *arrows* show different integration times used to monitor the observed signal.

The *drum illuminator* was used to calibrate both telescopes used in the *engineering array* test. The analysis of the *drum illuminator* calibration data for telescope-4 measured an average calibration of 4.0 ± 0.3 photons/ADC.[17] This result is compared with the *piece-by-piece* estimates in Figs. 2 and 9.

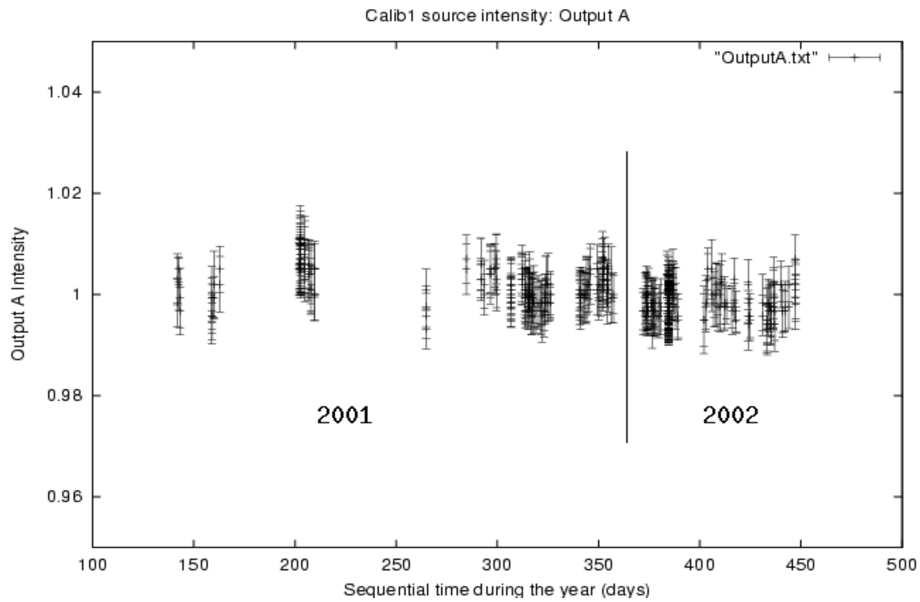

Figure 6. Optical calibration "A"-source intensity during the last year. The plot shows the light pulse intensities (average ± RMS) *versus* sequential day since January 1, 2001. The intensities are normalized to the average intensity for the entire time period.

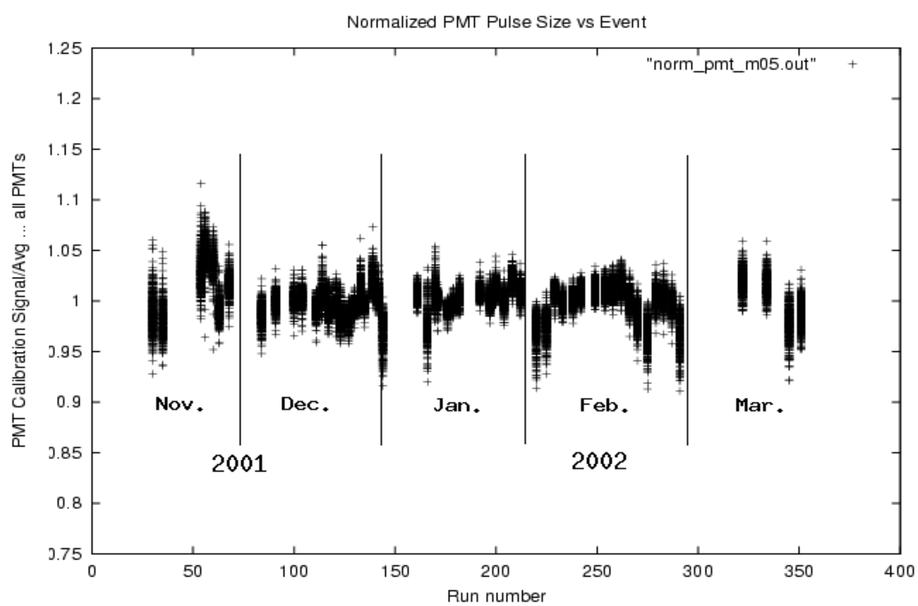

Figure 7. Time history of the *normalized* A-source calibration signals in all 440 pixels (PMTs) of telescope-5. As each pixel has a somewhat different signal, the vertical axis in the figure records each pixel's observed signal *normalized* by the average of that pixel's signal during the 5-month period. The horizontal axis is the sequential *run* number of each calibration. The vertical *smear* for each calibration run shows that the gains of individual pixels changed in time in comparison to the average (coherent) pixel trends. The vertical motion of the centroid of each *smear* shows that there were some coherent time variations of the pixel gains.

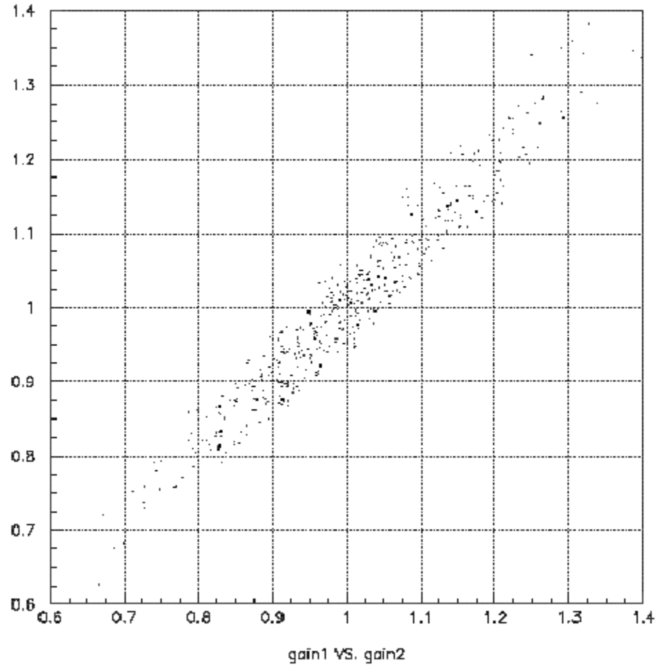

Figure 8. Plot of relative pixel gains using A-source calibration observed mean intensity (vertical axis) *versus* the ratio of observed variance/mean intensity (horizontal axis) for telescope-5. A special calibration run (with 850 events) was used for the variance/mean measurement.[12]

2.2. Relative Optical Calibration

The relative optical calibration system was used to monitor time variations in the telescope calibration between absolute calibrations. This was done with three xenon flash lamp[19] light sources coupled to optical fibers[20] to distribute light signals to three different destinations (denoted A, B and C) on each telescope; see Fig. 1. Source "A" signals terminated at 1-mm thick Teflon diffusers at the center of the mirror with the light directed at camera. Source "B" signals terminated at 1-mm thick Teflon diffusers at the center of two sides of the camera with the light directed at the mirror. Source "C" signals went to ports on the sides of the entrance aperture where the light was directed at reflective TYVEK targets mounted to the telescope doors where it was then reflected back into the telescopes.

Each calibration light source included a xenon flash lamp[19] at the focus of a f/1.5 lens, quartz beam splitter (to a monitoring fiber), filter wheel[21] and f/2.4 lens focusing onto a 1:7 optical fiber splitter.[22] Quartz optics were used through-out. A photo of one of the sources is shown in Fig. 4. One fiber from the 1:7 splitter was monitored[24]; the other six went to the six telescopes at a given fluorescence detector site.

The A-source included a Johnson-U filter[25] that approximated the wavelength acceptance of the fluorescence telescopes (Fig. 2) and a filter wheel with 5 different neutral density filters[26] that provided a dynamic range of ~ 100. Light pulses from the A-source are shown in Fig. 5. The B-source included only the Johnson-U filter. The C-source included a filter wheel with 5 different interference filters[26] to monitor stability at wavelengths of: 330nm, 350nm, 370nm, 390nm and 410nm.

The xenon light pulses were very stable with an RMS/average-pulse-intensity of $\sim 0.5\%$ for typical 50-pulse calibrations. Over many months of operation the xenon calibration pulses varied by $\sim 1\%$; see Fig. 6.

A-, B- and C- calibrations were taken at least once per night of fluorescence data taking. As the light sources were essential constant, cf. Fig. 6, the A-source calibration signals in each pixel (of each telescope) provided

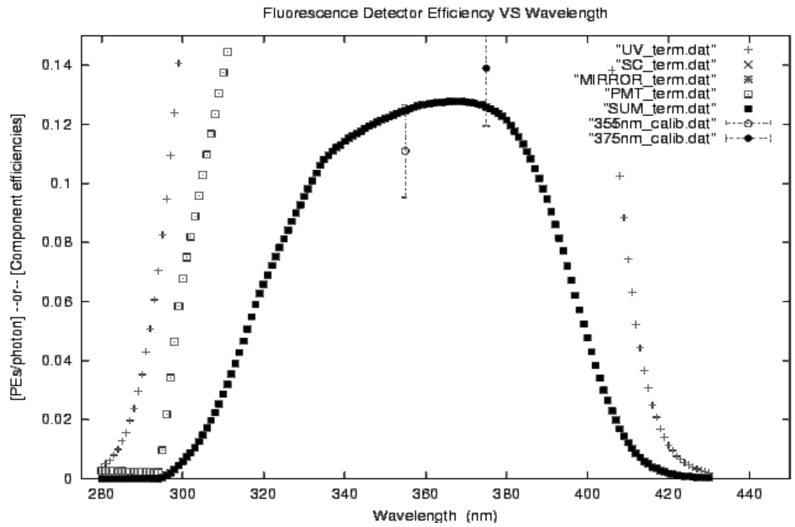

Figure 9. Expanded vertical scale version of Fig. 2 showing more clearly the comparison of the *piece-by-piece* (solid-box points), *Rayleigh* ("o"-point with error-bars) and *drum illuminator* ("•"-point with error bars) calibration results. The plot shows the predicted efficiency, $\epsilon_{PE}(\lambda)$, for producing a photo-electron per incident photon *versus* wavelength for Auger telescope-4. The (preliminary) gain $g = 1.8 \pm 10\%$ ADC/PE is used to plot the *Rayleigh* and *drum illuminator* absolute calibration results, points with error-bars, on this figure.

a monitor of the pixel stability. A plot of the signals for telescope-5 is shown in Fig. 7. The relative pixel to pixel variations with time, and the coherent variations with time, were typically $< 5\%$, cf. Fig. 7.

The A-source calibration data were also used to measure the relative pixel gains. This was done in two ways. The first approach used a semi-empirical model to correct for the position dependences of the light intensity at each pixel (from the diffuse light A-source on the optical axis of the camera). The corrected signal in each pixel was then a direct measure of the pixel gain. The average (corrected) signal was divided out so that the average relative gain was 1.0. The second approach used the pulse-to-pulse variations in the observed signal as a measure of the number of photo-electrons[12] in a given pixel. In practice the signal variance must be corrected for additional PMT-multiplication variations at the first dynode. The gain, in ADC/photo-electron, for the i^{th} pixel in the j^{th} telescope was then given by[12]:

$$g_{i,j} = \frac{\sigma^2_{i,j}}{\overline{ADC}_{i,j} \cdot 1.41} \qquad (2)$$

where $\sigma^2_{i,j}$ was the pixel signal variance and $\overline{ADC}_{i,j}$ was the pixel signal mean. Again relative gains were normalized to an average gain of 1.0. A comparison of the relative pixel gains from the two procedures is shown in Fig. 8. The agreement was typically better than 5%.

3. SUMMARY

The Auger *engineering array* test provided an opportunity to evaluate the proposed fluorescence detector calibration procedures, associated hardware and software. The three calibration procedures gave commensurate results at about the 20% level; see Fig. 9. Work is ongoing to improve each of the procedures and we expect consistency with better accuracy in the future. A natural benefit of our program of calibration studies was that calibrated data, see *e.g.* Fig. 10, were available early in the *engineering array* test for *hybrid* event analyses.

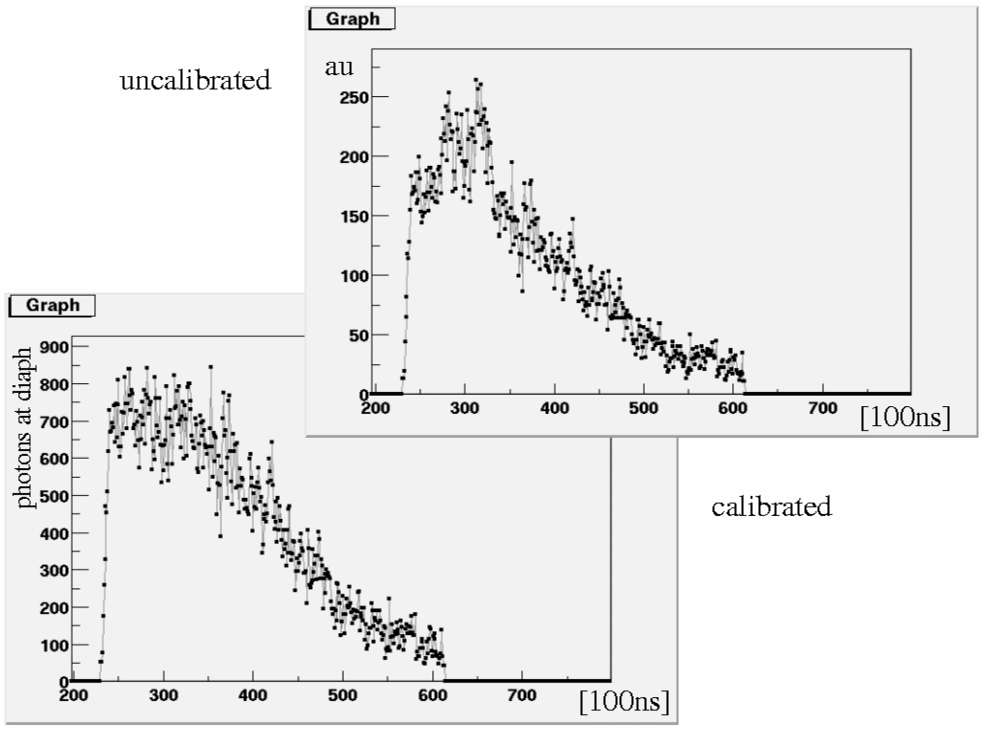

Figure 10. Example of cosmic ray air shower observed by the Auger fluorescence telescopes. The raw data are shown in the upper figure and are in ADC units. The calibrated data are shown in the lower figure and are in photon units (*i.e.* 360nm photons incident on the telescope aperture). This event happened to pass over many pixels with gains that were rather far from the average pixel gain of ~ 5 photons/ADC.

ACKNOWLEDGMENTS

The author would like to acknowledge the support of the U.S. Department of Energy (High Energy Physics Division) for funding this research under grant DE-FG03-92ER40732.

REFERENCES

1. J.A.J. Matthews, *New Results on the Highest Energy Cosmic Rays*, 200^{th} Meeting of the American Astronomical Society, Albuquerque, NM, June 3, 2002: http://www-hep.phys.unm.edu/~johnm/talk_aas.ps.gz
2. A. Etchegoyen, et al, *Layout of the Pierre Auger Observatory*, Proc. of 27^{th} Inter. Cosmic Ray Conf., **2**, 703 (2001).
3. B. Dawson, et al, *The Hybrid Aperture and Precision of the Auger Observatory*, Proc. of 27^{th} Inter. Cosmic Ray Conf., **2**, 714 (2001).
4. J.A.J. Matthews, et al, *Atmospheric Monitoring for the Auger Fluorescence Detector*, Proc. of 27^{th} Inter. Cosmic Ray Conf., **2**, 745 (2001);
   J.A.J. Matthews, et al, *Fluorescence Detector Optical Calibration and Atmospheric Monitoring for the Pierre Auger Experiment*, Auger note: GAP-2000-033 (2000) available at: http://www-hep.phys.unm.edu/~johnm/jpg_draft.ps
5. F. Kakimoto, et al, *A Measurement of the Air Fluorescence Yield*, Nucl. Instr. Meth. **A372**, 527 (1996); A.N. Bunner, *Ph.D. Thesis*, Cornell University, Ithaca, NY (1964).

6. G. Borreani, et al, *The Fluorescence Detector Prototype for the Auger Project: Mechanical Structure, Optical System and Filter*, Proc. of IEEE Trans, Nucl. Sci. **48**, 406 (2001);
G. Matthiae, et al, *Optics and Mechanics of the Auger Fluorescence Detector*, Proc. of 27^{th} Inter. Cosmic Ray Conf., **2**, 733 (2001);
H. Gemmeke, et al, *The Auger Fluorescence Detector Electronics*, Proc. of 27^{th} Inter. Cosmic Ray Conf., **2**, 737 (2001).
7. M-UG 6 special filter glass, 3.25mm thick, from Schott DESAG.
8. P. Facal San Luis and P. Privitera, *Measurement of the FD Camera Light Collection Efficiency and Uniformity*, Auger Note: GAP-2000-010 (2000) available at: http://www.auger.org/admin/GAP_Notes/index.html
9. Ultra CFR-GRM-THG-WS Pulsed Nd:YAG laser with frequency tripling to 355nm, optimized for 4Hz operation, 6mJ/pulse at 355nm from Big Sky Laser Technologies Inc., 601 Haggerty Lane, P.O. Box 8100, Bozeman, Montana 59715.
10. T. Tessier, et al, *Measurement of the Aerosol Differential Scattering Cross Section using HiRes Fluorescence Telescopes*, Proc. of 26^{th} Inter. Cosmic Ray Conf., **5**, 408 (1999).
11. NSHU550 UV LED, 1mW optical output, from Nichia America Corp., 181 Metro Drive, Suite 350, San Jose, CA 95110.
12. A. deCapoa, *Calibration of the FD Telescope Channels using Light Pulses*, Auger Note: GAP-2002-005 (2002).
13. H. Gemmeke, *Talk*, Auger Collaboration Meeting, April 22 - 26, 2002, Malargue, Argentina.
14. Rm-3700 single channel universal radiometer with RjP-734 5cm^2 cavity pyro-electric energy probe from Laser Probe Inc., 23 Wells Ave., Utica, NY 13502.
15. B. Dawson, et al, *An Absolute Calibration of the Bay 4 Telescope using Remote Laser Shots on October 20, 2001*, Auger Note: GAP-2002-010 (2002).
16. M. Roberts, *Talk*, Auger Collaboration Meeting, April 22 - 26, 2002, Malargue, Argentina.
17. J. Brack, et al, *Prototype Auger Absolute Calibration System: Fluorescence Detector Calibration at Los Leones*, Auger Note: GAP-2002-033 (2002).
18. P. Privitera, *Talk*, Auger Collaboration Meeting, April 22 - 26, 2002, Malargue, Argentina.
19. LS-1130-4 1100 Series FlashPac with FX-1160 xenon flash-lamp with reflector and borosilicate window from Perkin Elmer Opto-electronics, 35 Congress St., Salem, MA 01970.
20. 40m optical fiber patch cords, UV graded, 200 micron core, 0.22NA fibers from RoMack Inc., 105 Edward Wyatt Drive, Williamsburg, VA 23188.
21. AB301-T filter wheel from CVI Spectral Products Division, 200 Dorado Place SE, P.O. Box 11308, Albuquerque, NM 87192.
22. 1:7 fiber optic beam splitters, UV graded, 200 micron core, 0.22NA fibers from InnovaQuartz Inc., 4420 South 32nd Street, Phoenix, AZ 85040.
23. 18" $\times$ 30" optical bread-boards from Vere Inc., P.O. Box 777, New Kensington, PA 15068.
24. Rm-3700 single channel universal radiometer with RjP-465 silicon energy probe with UV-enhanced response from Laser Probe Inc., 23 Wells Ave., Utica, NY 13502.
25. XBSSL/U/25R, 1" diameter, Johnson/Cousins (Bessel) U-band filter from Omega Optical Inc., P.O. Box 573, Brattleboro, VT 05302.
26. Metallic neutral density filters and $\pm$5nm interference filters from Andover Corp., 4 Commercial Drive, Salem, NH 03079-2800.